

Design and Implementation of an Active Power Filter Using Model Predictive Controller

Mohammad Haeri, and Mahdi Zeinali

Advanced Control System Lab., Electrical Engineering Department,
Sharif University of Technology, Azadi Ave., Tehran, IRAN
(Tel: +98-21-616-5964; E-mail: haeri@sina.sharif.edu)
(Tel: +98-21-616-5971; E-mail: zeinali@mehr.sharif.edu)

Abstract: A parallel active power filter is designed and implemented to compensate for undesired current harmonics generated by a nonlinear load. The filter works based on PWM strategy and control signal is generated using a model predictive controller. To evaluate the achievements, a PI controller is also designed and implemented. Experimental results indicate about 50% increase in the efficiency over PI controller.

Keywords: Model predictive control, Active power filter, Current harmonic cancellation, PI controller

1. INTRODUCTION

Nonlinear loads such as electrical arc furnaces, AC/AC and AC/DC converters, saturating devices like transformers and electrical machines, discharging elements like fluorescent and incandescent lamps, and so on impose unwanted phenomenon on the power networks among them undesired current and/or voltage harmonics are more noticeable. These not only increase the losses of the power in the network, but also cause damages on sensitive loads such as micro controllers/micro processors and produce noise in control circuits including those in power generating stations [1]. Two different methods are usually employed to compensate for the undesired harmonics. Use of the passive RLS filters was the first approach in this regard. Due to the existing limitations on the achievable performance of these filters, active filters have find wide application in recent years [2]. In general, an active filter is equivalent to a dependent current/voltage source. A parallel (shunt) active filter, which is used to eliminate current harmonics, contains a DC voltage source, a switching circuit and an impedance. A PWM voltage inverter derives the switching circuit. Different control strategies have so far been used to determine the input signal for PWM converter.

In this work, we examine efficiency of a special model predictive controller called generalized predictive controller (GPC) [3]. To evaluate the results we apply a standard PI controller as well. A simple nonlinear load (AC/DC converter), which produces current harmonics, is implemented. Performances of the controllers are compared in different situation including mismatch in the nonlinear load and mismatch in active filter impedance.

Experimental results indicate an increase of about 50 % improvement in the active filter performance when a predictive controller is implemented.

The paper is organized as follows. In Section 2, active power filter and its related control loops are introduced. In Section 3, design of model predictive and PI controllers are discussed. Section 4 describes test bed circuitry of the experiment. Experimental results are given in Section 5 and finally paper concluded in Section 6.

2. ACTIVE POWER FILTER

The active power filter, which is used to remove the harmonics of the current, is a controllable current source. Decrease of the current harmonics level is done by infusion a current with specific amplitude and phase into the line. The

produced current, follows a given reference signal. If the load current is denoted by $I_{ld}(t) = I_{l1}(t) + I_h(t)$, where $I_{l1}(t)$ is the 50 Hz component and $I_h(t)$ is the total sum of the other harmonics, then one can remove the undesired harmonics from the source voltage generator by defining the reference signal as $I_{ref}(t) = I_h(t)$. In other words, after the compensation, the voltage source will have only the 50 Hz current component, which is in the same phase with the source voltage. The active filter provides the undesired harmonics of the load current as well as its reactive power. The main component of the load current can be obtained using an appropriate filter.

The active filter current $I_{gen}(t)$ is generated by a PWM voltage inverter and an impedance $Z(s)$ (Fig. 1). Fig. 2 shows the block diagram of the active filter.

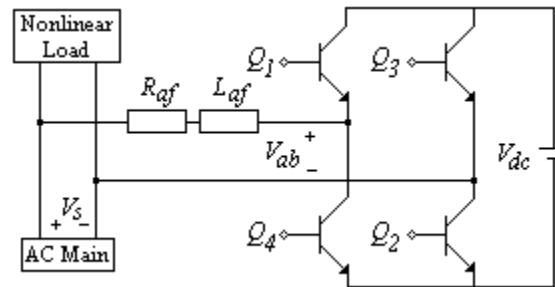


Fig. 1. Circuitry of the active filter.

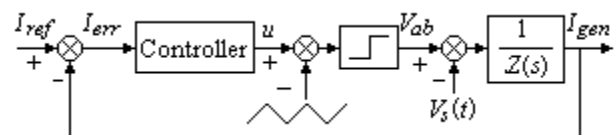


Fig. 2. Block diagram of the active filter.

The computational period of active filter is T_s . At the beginning of each computational period, the controller determines the control signal u and then the appropriate switches from the inverter are turned on for a specific time. This is done by comparing the control signal u with a triangular wave signal. The frequency of this wave is $f_s = 1/T_s$. During each period T_s , when the value of u is

greater than the instantaneous value of triangular wave, switches Q_1 and Q_2 are on and voltage $+V_{dc}$ is appeared at the inverter output. At the time, which the value of u is smaller than the instantaneous value of triangular wave, switches Q_3 and Q_4 are on and voltage $-V_{dc}$ is appeared at the inverter output. Amplitude of u is normalized between 0 and 1.

As can be seen from Fig. 1, voltage drop across the impedance $Z(s)$ is $V_{ab}(t) - V_s(t)$. This produces current in the impedance that contains different harmonic components. By controlling $V_{ab}(t)$, harmonics of the current can be controlled in such way that it tracks the reference current.

3. CONTROLLERS

As shown in the Fig. 2, the input u is determined by the controller so that the output current of the filter ($I_{gen}(t)$), follows the $I_{ref}(t)$. The source voltage $V_s(t)$ is treated as the external disturbance. Combination of the inverter and the impedance is considered the system that should be controlled. the following control laws are examined.

3.1 PI controller

A discretized form of the PI controller is;

$$u(t) = u(t-1) + k_p \left\{ (1 + T_s/T_i) I_{err}(k) - I_{err}(t-1) \right\} \quad (1)$$

T_i , k_p are the design parameters. k_p determines slowness/fastness of the closed-loop system. Increase of k_p leads to speedy closed-loop system. However, for larger value of k_p , the control signal becomes large as well. The control signal should be always in the range of the triangular wave magnitude. Otherwise it causes malfunctioning of the PWM converter. Here it is assumed that $0 < u(t) < 1$. If k_p becomes smaller, the closed-loop system is slow and the generated current won't be able to follow the reference signal. T_i determines the damping of the system. The large value of T_i won't decrease the undesired harmonics level.

3.2 Generalized predictive controllers

Generalized Predictive Controller (GPC) belongs to the model predictive control family. A transfer function model of the system is used in this controller to predict the future outputs of the system. The control signal is computed according to this fact that the future response of the system should track a desired output trajectory. Usually the following cost function is used.

$$J = \sum_{k=n_1}^{n_1+P} (y_d(t+k) - y(t+k))^2 + r \sum_{k=1}^M (\Delta u(t+k-1))^2 \quad (2)$$

r indicates the relative importance of two terms in the cost function. Usually a first order filter is used to make the reference signal smooth enough and determine the desired output.

$$\begin{aligned} y_d(t) &= y(t) \\ y_d(t+k) &= \alpha y_d(t+k-1) + (1-\alpha)y_s(t), \quad k=1,2,\dots,P \end{aligned} \quad (3)$$

$y_s(t)$ is the reference signal at the sample time t and α is the filter parameter and determines the smoothness of the desired output signal. α is selected between 0 and 1. The larger value of α makes the desired output more smother. P is the prediction horizon and indicates time duration in which the system output is considered in the optimization. It's assumed that the control signal u can be changed only in the first M steps, and then become fixed. M is called the control horizon. P should be sufficiently large in order to include the transient state of system. If P is chosen very large, then the initial errors will have less effect in the cost function. Increasing the magnitude of P leads to stability of the closed loop system.

The following relation gives output of the system at sample time $t+k$.

$$\begin{aligned} \hat{y}(t+k|t) &= \sum_{i=1}^k g_i u(t+k-i) + y_{past}(t+k|t) + \hat{n}(t+k|t) \\ k &= 1, 2, \dots, P \end{aligned} \quad (4)$$

g_i is the step response coefficients of the system. The first term of (4) includes the future variations of the input signal (should be determined) and the next term is the free response of the system at sample time $t+k$ that is because of variation of the input signal in the previous sample times. The third term indicates external disturbances as well as the model process mismatch. Usually a simple estimation of this term is employed which is a constant equal to difference between model and system outputs at sample time t . Equation (4) is rewritten in compact form as follows.

$$Y = G\Delta u + Y_{past} + D \quad (5)$$

G is the dynamic matrix of the system. The purpose of the control is to find $\Delta u = [\Delta u(t), \Delta u(t+1), \dots, \Delta u(t+M-1)]^T$ so that the cost function J become minimized. The cost function in the matrix form is;

$$J = (Y_d - Y)^T (Y_d - Y) + r \Delta u^T \Delta u \quad (6)$$

Y_d is the desired output (filtered reference signal). The minimum of J is obtained for the following input signal variations.

$$\Delta u = (G^T G + rI)^{-1} G^T (Y_d - Y_{past} - D) \quad (7)$$

Usually, the first element is used to determine the control signal.

$$\Delta u(t) = [1 \ 0 \ \dots \ 0] K_{GPC} E = k_{GPC} E \quad (8)$$

Consequently, the input is derived as,

$$u(t) = u(t-1) + \Delta u(t) \quad (9)$$

In order to apply this controller, k_{GPC} is calculated off-line once in the beginning of the simulation. E is calculated on-line in each sample time.

4. NONLINEAR LOAD DESCRIPTION

As a load we used a diode rectifier AC/DC converter system with $L = 3 \mu H$, $C = 330 \mu F$, and $R = 32.3 \Omega$ (Fig. 3). Amplitude of the source voltage is $6.6 v$ and switching frequency considered being $30 KHz$. As this frequency increases, we get better results. Impedance $Z(s)$ comprises from $L_{af} = 40 mH$, $R_{af} = 102.3 \Omega$, and $V_{dc} = 12.5 v$.

A filter has been used to generate the reference current. Since it leads to a delay, this is considered in design stage of the controller. In the practical test, the controller and the mentioned filter have been implemented in SIMULINK and the rest of the circuit including active filter, inverter PWM, nonlinear load and source voltage has been constructed on the breadboard. The load current is measured online and converted to discrete signal through an AD/DA and is accessible by the SIMULINK. This signal is passed through a low-pass filter to generate the reference signal. The difference of this signal and the one produced by the active filter is also available for SIMULINK through the AD/DA card. The control signal is computed in SIMULINK and made available on the output port of the same card. The control output is compared with the triangular wave magnitude. If the control signal is greater, then output of the comparator becomes high. Otherwise it becomes low. This output is connected to the base of four transistors directly or through NOT gates. In this way, if the value of u is greater than the triangular wave magnitude, the switches Q_1 and Q_2 become on and $+V_{dc}$ is appeared in output, if the value of u is less, than the switches Q_3 and Q_4 become on and $-V_{dc}$ is appeared in the output.

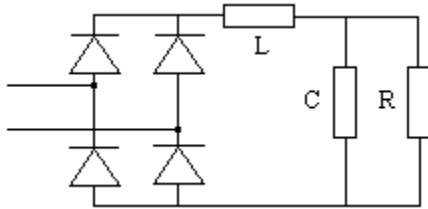


Fig. 3. Nonlinear load circuitry.

5. EXPERIMENTAL RESULTS

The following relation gives an approximated model for the active power filter.

$$G(s) = \frac{2V_{dc}e^{-T_d s}}{Z(s)} \quad (10)$$

T_d represents delay time produced by the comparator and NOT gates due to their limited bandwidth. Use of the parameters value in (10), the following first order plus delayed time model is obtained.

$$G(s) = \frac{ke^{-T_d s}}{\tau s + 1} = \frac{0.2444e^{-0.005 s}}{3.91 \times 10^{-4} s + 1} \quad (11)$$

To design PI controller, Cohen-Coon method is employed [4].

$$K(s) = k_c \left(1 + \frac{1}{T_i s} \right)$$

$$k_c = \left(0.9 \frac{\tau}{T_d} + 0.083 \right) / k \quad (12)$$

$$T_i = \tau \left(3.33 \frac{T_d}{\tau} + 0.31 \left(\frac{T_d}{\tau} \right)^2 \right) / \left(1 + 2.222 \frac{T_d}{\tau} \right)$$

This results in the following PI control parameters.

$$k_c = 0.6276, \quad T_i = 0.00124$$

The control parameters of the predictive controller are selected as,

$$M = 3, \quad r = 0.5, \quad \text{and} \quad \alpha = 0.5$$

The rising time of the system is around $t_r = 0.000859 \text{ sec}$ and therefore P is selected as 26. These are values that are commonly used in the implementation of GPC controller [3].

To evaluate the performance of the controllers, the *THD* (Total Harmonic Distortion) criterion is used. In general we can suppose $I(t)$ to be in the following form.

$$I(t) = I_1(t) + I_2(t) + \dots \quad (13)$$

In which $I_j(t)$ is the j^{th} harmonic component of the signal. Thus *THD* is defined as below.

$$THD = \frac{\sqrt{I_2^2 + I_3^2 + \dots}}{I_1} \times 100 \quad (14)$$

Current of the nonlinear load, which is described in the previous section, is depicted in Fig. 4. The frequency spectrum of the current is shown in Fig. 5. *THD* is 40% in this case.

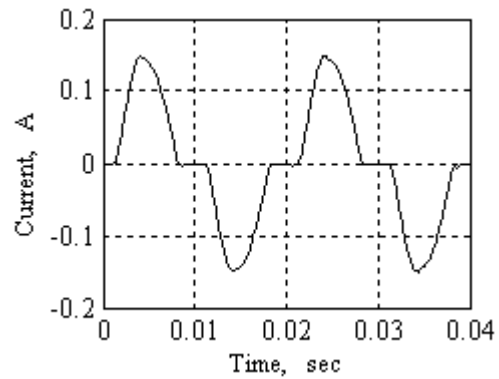


Fig. 4. The load current.

When the controllers are applied, the source current is changed from the one in Fig. 4 to that in Fig. 6 for PI and Fig. 7 for GPC controllers. The frequency spectra of the source current are shown in Figs. 8 and 9 for PI and GPC controllers respectively. Using these controllers *THD* has been reduced to 13.36% and 5.76% respectively. This shows good performance achievement with regard to *THD* cancellation

5.1 Mismatch in active power filter impedance

At this stage, we investigate robustness of the controllers. To do so, we add a 20Ω resistance in series with the existing

102.3 Ω resistance of the active filter. This is equivalent to introduce some 20 % mismatch between model and the system. Since the nonlinear load has not been changed, the source current *THD* is still 40%. When the controllers are applied to the system, the source current becomes what is shown in Fig. 10 for the PI and in Fig. 11 for GPC controllers. The frequency spectra of the currents are given in Figs. 12 and 13 respectively. Using PI controllers, *THD* decreased to 15.71% and using GPC it becomes 6.1%. As it is expected, the performance has been degraded. However, it is not that much noticeable.

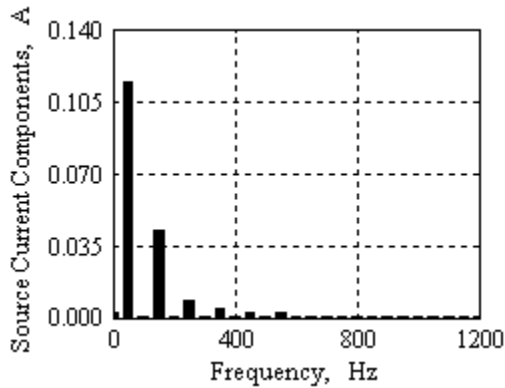


Fig. 5. Frequency spectra of the load current.

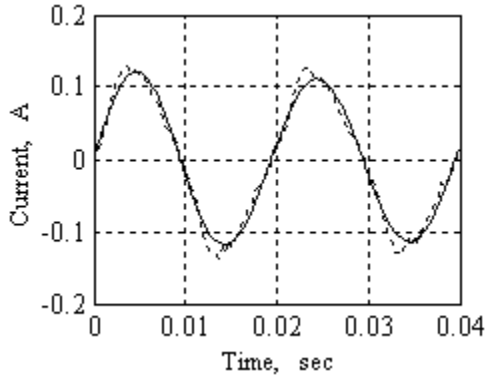


Fig. 6. Source current with PI controller.

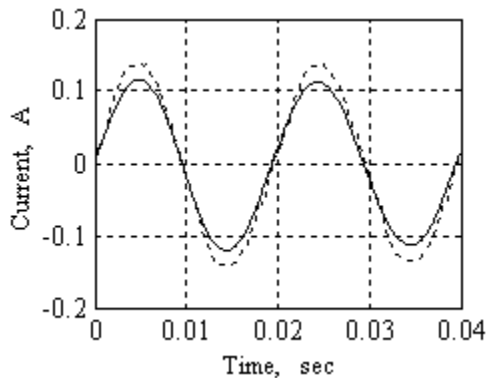


Fig. 7. Source current with GPC controller.

5.2 Mismatch in nonlinear load

The nonlinear load acts like a source of the external disturbance for the system. We replaced the existing resistance

32.3 Ω by a 83.5 Ω resistance. This means an increase of 158.5%, which will obviously changed the source current characteristics. *THD* of the source current is changed from 40% in the previous case to 60% in this case. The load current is depicted in Fig. 14 and its frequency spectrum is shown in Fig. 15.

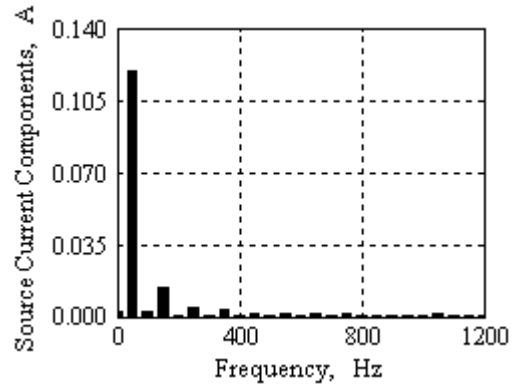


Fig. 8. Frequency spectra of the source current using PI controller.

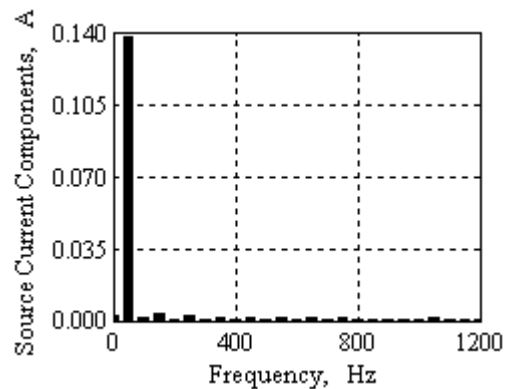


Fig. 9. Frequency spectra of the source current using GPC controller.

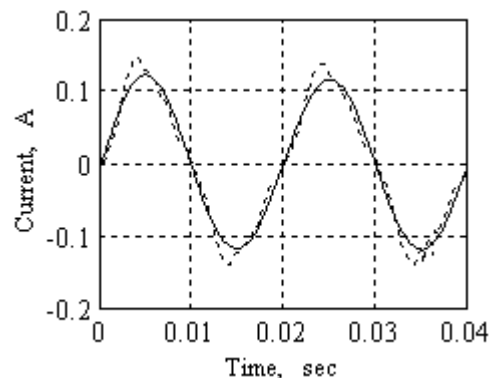


Fig. 10. Source current using PI controller.

Figs. 16 and 17 show the source current after application of the PI and GPC controllers. The frequency spectra of the current are given in Figs. 18 and 19 as well. Usage of the controllers decreases *THD* to 18.64% and 6.8% for the PI and GPC controllers respectively. In this case the performance is degraded as well however it is acceptable compared to the magnitude of the changes in the load resistance.

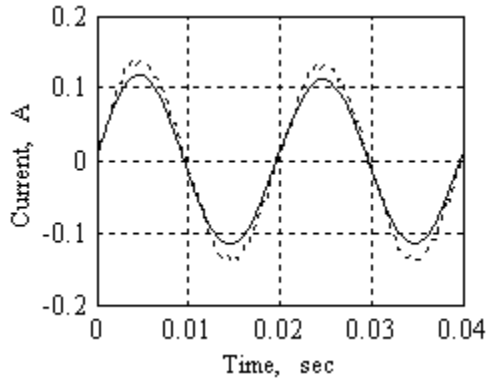


Fig. 11. Source current using GPC controller.

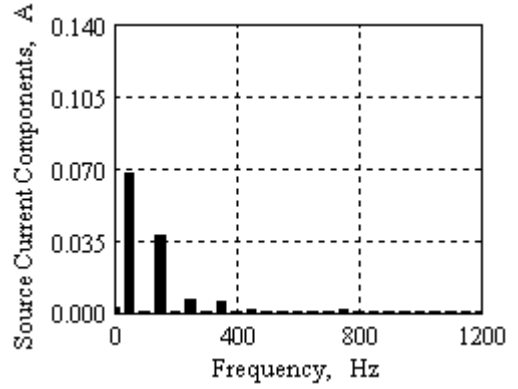


Fig. 15. Frequency spectra of the load current.

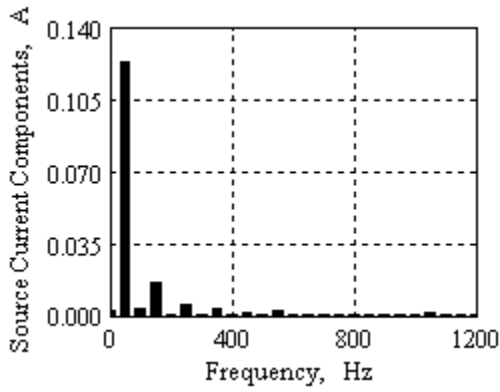


Fig. 12. Frequency spectra of the source current using PI controller.

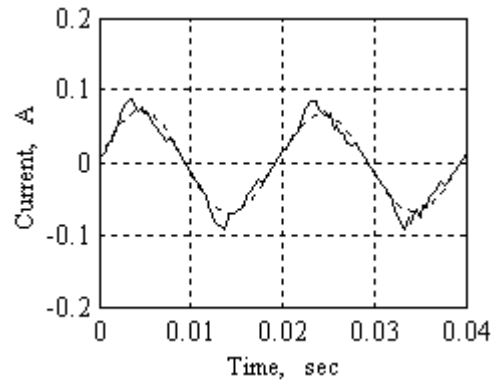


Fig. 16. Source current using PI controller.

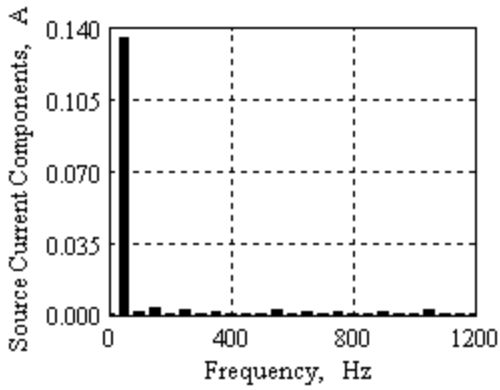


Fig. 13. Frequency spectral of source current using GPC controller.

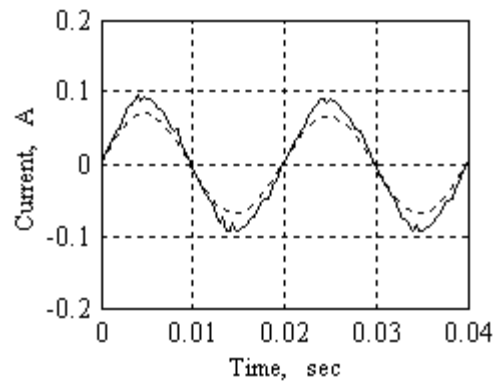


Fig. 17. Source current using GPC controller.

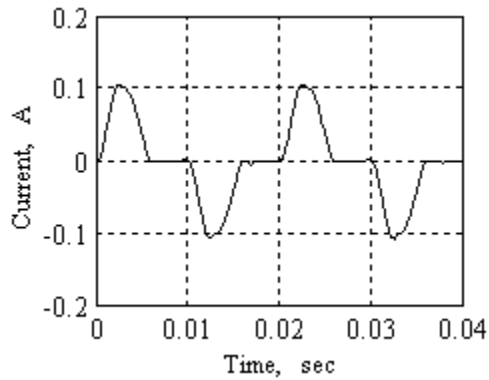


Fig. 14. Load current.

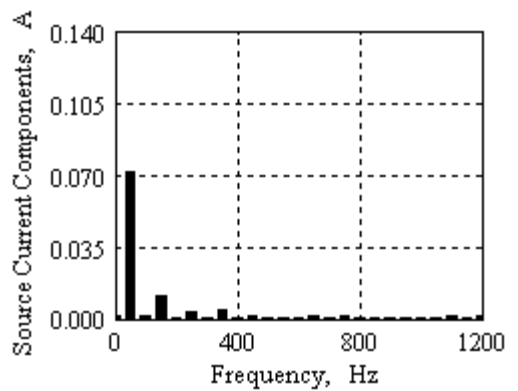


Fig. 18. Frequency spectral of source current using PI controller.

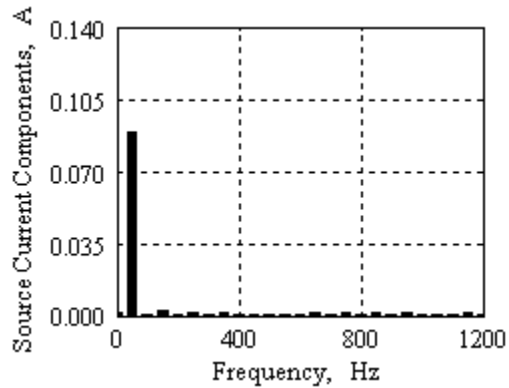


Fig. 19. Frequency spectral of the source current using GPC controller.

6. CONCLUSIONS

The GPC controller indicates better performance in all three implementations compared to those of the PI controller. In the last two implementations, the performance of the controllers is worth than that of the nominal case. However, referring to an increase about 20 % in the system dynamics or 160 % in the load dynamics, this matter can be rationalized. In both cases, the rate of *THD* increase is less for the GPC controller than that of the PI controller.

ACKNOWLEDGMENTS

Financial support from Sharif University of Technology is gratefully acknowledged.

REFERENCES

- [1] R.C. Dugan, M.F. McGranaghan, and H.W. Beaty, *Electrical power systems quality*, McGraw-Hill, 1996.
- [2] L.A. Moran, J.W. Dixon, and R.R. Wallace, "A three-phase active power filter operating with fixed switching frequency for reactive power and current harmonic compensation", *IEEE Transactions on Industrial Electronics*, Vol. 42, No. 4, pp. 402-408, Aug. 1995.
- [3] E.F. Camacho and C. Bordons, *Model predictive control in the process industry*, Springer, 1995.
- [4] K. Astrom and T. Haggglund, *PID controllers: theory, design and tuning*, 2^{ed} Ed., Instrument Society of America, 1996.